




Sustained release system of paclitaxel based on composite nanofibers for inhibiting renal clear cell carcinoma

Zhiduan Cai^{1,2}, Haoquan Zhuang^{1,2}, Xiezhao Li^{1,2}, Siyang Liang^{1,2}, Wenjun Luo^{1,2}, Yaoji Yuan^{1,2}, Yuyu Xu^{1,2}, Lin Jin^{1,2,4,*}, and Guibin Xu^{1,2,3,*} 

¹Department of Urology, Key Laboratory of Biological Targeting Diagnosis, Therapy and Rehabilitation of Guangdong Higher Education Institutes, The Fifth Affiliated Hospital of Guangzhou Medical University, Guangzhou Medical University, Guangzhou 510700, China

²Guangzhou Key Laboratory of Enhanced Recovery After Abdominal Surgery, The Fifth Affiliated Hospital of Guangzhou Medical University, Guangzhou Medical University, Guangzhou 510700, China

³Guangdong Provincial Key Laboratory of Urology, The First Affiliated Hospital of Guangzhou Medical University, Guangzhou Medical University, Guangzhou 510230, China

⁴International Joint Research Laboratory for Biomedical Nanomaterials of Henan, Zhoukou Normal University, Zhoukou 466001, China

Received: 19 August 2022

Accepted: 31 October 2022

Published online:

16 November 2022

© The Author(s) 2022

ABSTRACT

The recurrence and metastasis of renal cell carcinoma are severe challenges in clinical treatment. At present, it is urgent to find a strategy to solve this problem and improve the therapeutic effect. In this study, we designed a programmed release system of anticancer drugs by preparing a nanofiber system with two kinds of diameters and biomaterials (polylactic acid-glycolic acid (PLGA) and silk protein) as drug carriers (paclitaxel), which inspired the occurrence and pathological microenvironment of renal cell carcinoma. The controlled degradation of PLGA nanofibers as a drug carrier achieved the short-term release of paclitaxel, which could rapidly inhibit the spread and metastasis of renal cancer, while the silk protein nanofibers as a drug carrier with slow degradation could provide the long time and continuous release of paclitaxel to prevent the proliferation of renal cancer cells and inhibit recurrence. The synergistic effect of the sustained release system of paclitaxel successfully achieved inhibition of the recurrence and metastasis of renal cell carcinoma and improve the therapeutic effect of renal cell carcinoma. The paclitaxel release profile showed that the PLGA nanofiber drug system provided controlled release of paclitaxel in the first 14 days, while the silk protein nanofiber system provided a relatively stable and long-duration release of

Handling Editor: Annela M. Seddon.

Zhiduan Cai and Haoquan Zhuang have contributed equally to this work.

Address correspondence to E-mail: jinlin_1982@126.com; uro_xgb@163.com

paclitaxel (1 month). In vitro experiments showed that the sustained release system of paclitaxel had a lasting inhibitory effect on the proliferation of renal clear cell carcinoma cells. These results indicated that the sustained release system of paclitaxel could be used as a promising drug delivery system with highly efficient implementations to reduce the frequency of systemic administration and inhibit tumor growth and recurrence, which could provide a new strategy for the clinical applications in renal cell carcinoma microenvironment.

Introduction

Cancer is a leading cause of premature death in the world [1]. According to estimates by the World Health Organization in 2019, cancer is the first or second leading cause of death before the age of seventy in two-thirds of the countries in the world [2]. Renal cell carcinoma (RCC) accounts for approximately 2% of newly diagnoses cancer cases and cancer deaths in the world, particularly in developed countries. It is expected to cause about 76080 new cases and 13780 deaths in the USA in 2021 [3]. RCC is the most common renal malignant tumor, and approximately 75% of renal cancer cases are renal clear cell carcinoma (ccRCC) [4, 5]. ccRCC is named after how the appearance of the cancer cells, which look clear under the microscope. Localized renal cancer can be treated with a partial or radical nephrectomy to remove the kidney, but 30% of patients will eventually develop recurrence and metastases [6]. Metastatic ccRCC is insensitive to chemoradiotherapy and has a varied response to targeted therapy. Most patients will have a poor prognosis and high mortality [7–9]. Therefore, we need to develop new treatment strategies to improve the therapeutic outcomes of ccRCC.

Paclitaxel is one of the most common anticancer drugs and is effective against a variety of human tumors [10–12]. Paclitaxel inhibits the growth of cancer cells by promoting the assembly of tubulin into microtubules and preventing their dissociation, thereby, blocking the cell cycle process [13]. However, the lipophilic properties of paclitaxel make it difficult to dissolve in water. Lipid-based cosolvents need to be added for clinical use, such as polyoxyethylated castor oil, which can be associated with serious and dose-limiting toxicities [14, 15]. Immediate anaphylaxis (HSRs) occurs during or after paclitaxel infusion in 30% of patients [16]. The

12-step administration method, using three bags of serial tenfold dilutions, is the most widely used desensitization protocol which involves a slow exposure to the paclitaxel [17]. Albumin-bound paclitaxel is a new nanopreparation of paclitaxel that combines endogenous, human albumin with paclitaxel in a noncovalent form without a cosolvent. Therefore, it has the advantages of safety, nontoxicity, nonimmunogenicity, biodegradation, and good biocompatibility [18]. There are reports of a novel, nano-assembled, drug delivery system formed by multivalent host–guest interactions between polymer-cyclodextrin conjugates and polymer-paclitaxel conjugates, which efficiently delivers paclitaxel into the targeted cancer cells [19]. All of these systems are designed to improve the solubility and stability of paclitaxel. Yet, its systemic administration leads to an increase in local blood concentration, resulting in an increased incidence of adverse reactions. Recently, poly (ϵ -caprolactone), paclitaxel, and magnetic nanoparticles have been used to design a smart nanofiber system that combines chemotherapy and hyperthermia. Paclitaxel is released over a long interval and synergizes with hyperthermia to kill tumor cells [20]. As such, the development of new, local therapeutic strategies for cancer treatment may offer many advantages.

Biomaterials, such as polylactic acid–glycolic acid (PLGA) and silk proteins, are biocompatible and biodegradable and are considered as attractive candidates for the controlled/sustained release of drugs [21, 22]. Currently, PLGA, a polymer synthesized from lactic acid and glycolic acid, is one of the most successfully used biodegradable polymers. The lactic acid and glycolic acid produced by its hydrolysis can be metabolized by the tricarboxylic acid cycle, so it has the least systemic toxicity. It has been approved by both the Food and Drug Administration (FDA) and European Drug Administration for

use in a variety of human drug delivery systems [23, 24]. PLGA has different molecular weights and copolymer compositions, and the degradation time depends on the molecular weight and copolymer ratio [25]. Silk protein is a natural fibrin polymer produced by arthropods like silkworms and spiders. It has become a candidate material for biomedical applications due to its properties such as biocompatibility, biodegradability, and nonimmunogenicity, its slow rate of degradation *in vivo*, and its ability to be processed into a variety of materials from aqueous solutions to organic solvents [26]. Silk protein-based biomaterials have been used as sustainable drug delivery carriers for a variety of bioactive molecules, including genes, small molecules, and drugs [27–29].

Electrospinning is a widely available technique for producing ultrathin fibers. Electrospun fibers are commonly referred to as nanofibers when their diameters are less than 500 nm. A large number of biocompatible and biodegradable synthetic polymers, such as polylactic acid (PLA), and PLGA, have been directly electrospun into nanofibers and further explored as scaffolds for biomedical applications [30]. Electrospun nanofibers have a higher surface area to volume ratio, contributing to a larger contact area with cancer cells [31]. In addition, electrospun nanofibers can be easily loaded with drugs for their controlled release and local delivery, leading to more effective chemotherapy. In a study by Qi et al. [32], composite nanofibers were prepared by electrospinning by mixing doxorubicin with PLGA polymer solution, resulting in sustained release of doxorubicin for a long time, which effectively inhibited the growth of HeLa cells. In another study [33], injectable PH-sensitive silk protein nanofiber hydrogels were prepared by electrospinning to maintain doxorubicin release for 8 weeks, with long-term cytotoxicity to cancer cells *in vitro* and *in vivo*.

As shown in Scheme 1, considering the different properties and degradation properties of PLGA and silk protein, we prepared two kinds of nanofibers with different diameters as drug carriers by electrospinning. The two-level drug delivery system that we developed can satisfy either the short-term release or long-term sustained release of paclitaxel in a local area to inhibit tumor growth and recurrence. The results of our experiments showed that

the antineoplastic membranes with drug sustained release (ANM-DSRs) we developed achieved a long-term supply of paclitaxel and had a lasting inhibitory effect on the proliferation of renal clear cell cancer cells. Renal cell carcinoma is insensitivity to chemotherapy [34, 35] and the dose toxicity of chemotherapeutic drugs limits the frequency and dose of systemic administration. Therefore, the local, long-term, drug administration strategy used in this study provides a new treatment direction for cancer treatment and meets actual clinical needs [36].

Experimental section

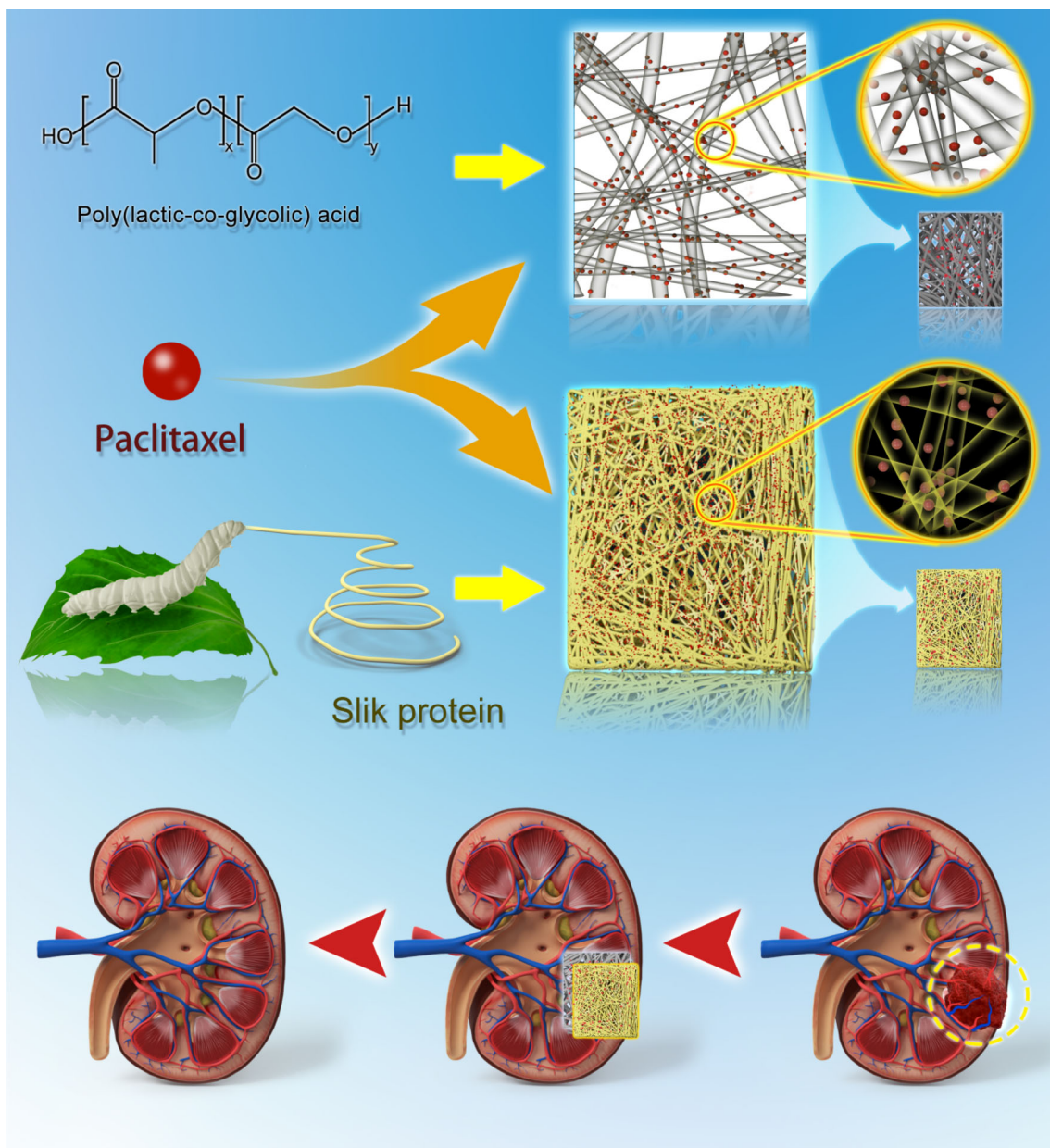
Materials

PLGA (MW = 100 kDa) was obtained from daigang Co (Jinan, China). The silk protein was prepared as described previous method [21]. Paclitaxel was purchased from Shanghai Ruiyong Biotechnology Co (Shanghai, China). All other chemicals were purchased from Guangzhou Chemical Co. (Guangzhou, China) and used without further purification.

Fabrication and characterizations of ANM-DSR

Fabrication of ANM-DSR

For ANM-DSR fabrication, PLGA (100 mg) and paclitaxel (2.0 mg) were dissolved in 1 mL composite solvent of dichloromethane and N,N-Dimethylformamide (V: V = 1: 9), and silk protein (100 mg) and paclitaxel (2.0 mg) were dissolved into the mixture of 1 mL formic acid and hexafluoroisopropanol (V: V) = 1: 9), respectively. Then the above-mixed solution was used to prepare the ANM-DSR by electrospinning process according to our previous method [21]. Briefly, the mixed solution was transferred into a syringe equipped with a needle nozzle (aperture: 0.5 mm; Yangzhou shuisi Co., Yangzhou, China). The speed was set as 0.5 mL/h using the syringe pump (Hebei Lange Co., Shijiazhuang, China). Meanwhile, a 16 kV electrical potential was provided by a high-voltage power supply. The ANM-DSR is collected by a flat collector between the tip of the needle and the collector at a distance of 15 cm.



Scheme 1 Two kinds of biomaterials were processed into nanofibers of different sizes to achieve short-term and long-term sustained release of paclitaxel for the treatment of renal cell

carcinoma. Scheme 1 is drawn using Photoshop (Adobe, San Jose, USA) and 3ds Max (Autodesk, San Rafael, USA) software.

Characterization of ANM-DSR

The morphology of ANM-DSR nanofibers was tested using the Quanta 200 scanning electron microscope (SEM, FEI, Netherlands; gas: nitrogen). After the ANM-DSR was mounted on the conductive adhesive

and sputtered with gold/palladium, the nanofibers were imaged under the accelerated voltage of 15 kV. The average diameter of nanofibers was quantified by the ImageJ software of the National Institutes of Health (Bethesda, USA).

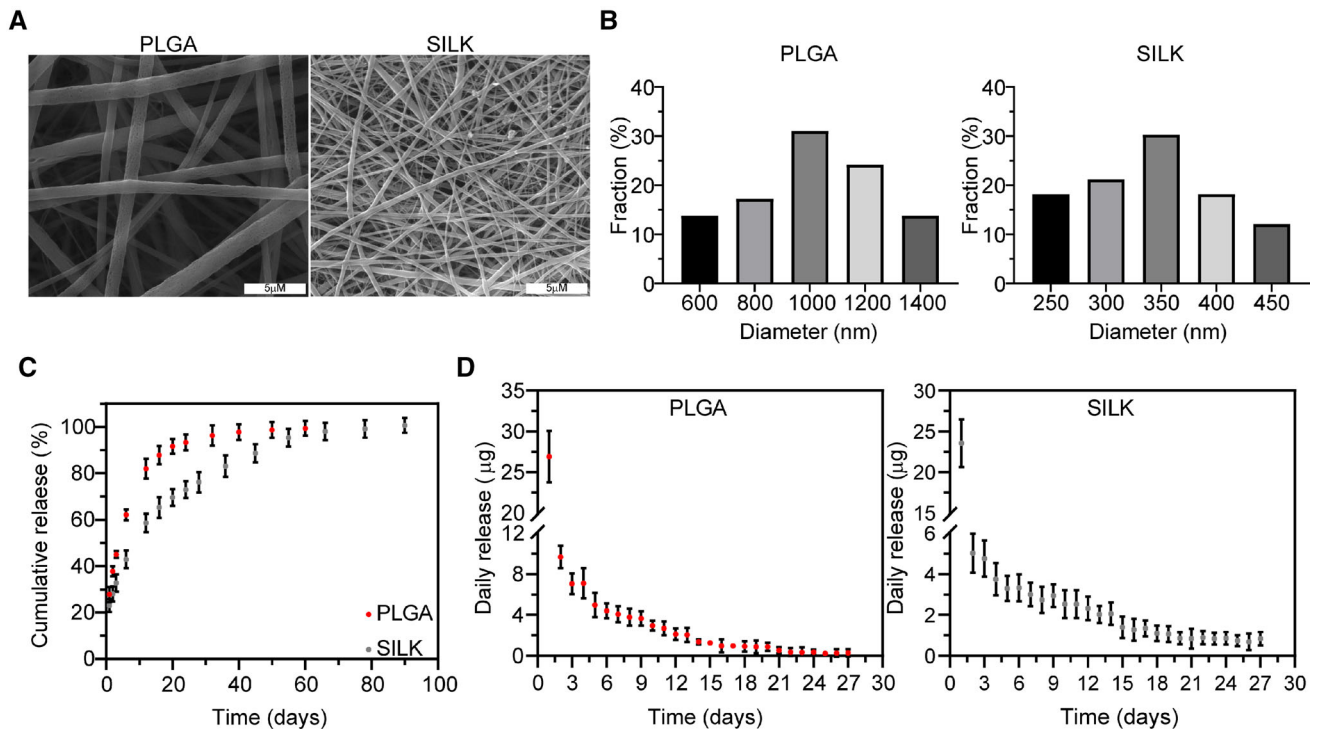


Figure 1 Biological characteristics and drug release profiles of ANM. **a** SEM image of the ANM of PLGA and silk protein. **b** Quantification of diameters of the ANM of PLGA and silk protein. **c** Average cumulative release profiles of paclitaxel from

the ANM of PLGA and silk protein in the whole process. **d** Average daily release amounts of paclitaxel from the ANM of PLGA and silk protein.

Determination of drug loading content and in vitro drug release

The drug loading of paclitaxel in ANM-DSR is defined as the weight percentage or mass of the drug in each membrane. To determine the drug loading, the pre-weighed freeze-dried membrane was re-dissolved in formic acid. The drug content was determined by an ultraviolet spectrophotometer. The release behavior of paclitaxel in ANM-DSR was determined by dynamic dialysis. The ANM-DSR was packed in a dialysis bag (MWCO:3.5 kDa), and the dialysate is transferred to a glass device containing 100 mL phosphate buffer solution (PBS) as a release medium. The glass instrument was then shaken at the rate of 100 rpm in an incubator at 37 °C. At the specified time point, 1 mL of solution outside the dialysis bag was replaced with the same amount of fresh PBS. The sample concentration was determined by measuring UV–Vis absorbance at 230 nm by an Epoch 2 microplate spectrophotometer (BioTek, Vermont, USA) [37]. The paclitaxel release was calculated according to the standard calibration curve of paclitaxel in PBS. The experiment was carried out in triplicate.

In vitro studies

Cell culture

Renal clear cell carcinoma cell line 786O was purchased from the cell bank of the China Center for Type Culture Collection (Shanghai, China). 786O was cultured in 1640 medium containing 10% fetal bovine serum, 100 IU/mL penicillin, and 100 µg/mL streptomycin (Gibco, Grand Island, USA) in an incubator (Thermo, Waltham, USA) at 37 °C and 5% carbon dioxide.

Live/dead cell analysis

The ANM-DSR and blank membranes were cut into 7*7 mm² slices and adhered to the carry sheet glass. After UV irradiation, the carry sheet glass was placed in 24-well plates. The cells were seeded on the carry sheet glass with a density of 50000 cells per well and cultured for 1–3 days. Every day, the cells were stained with calcein-AM and PI (Meilunbio, Dalian, China) at 37 °C for 30 min. The images were obtained

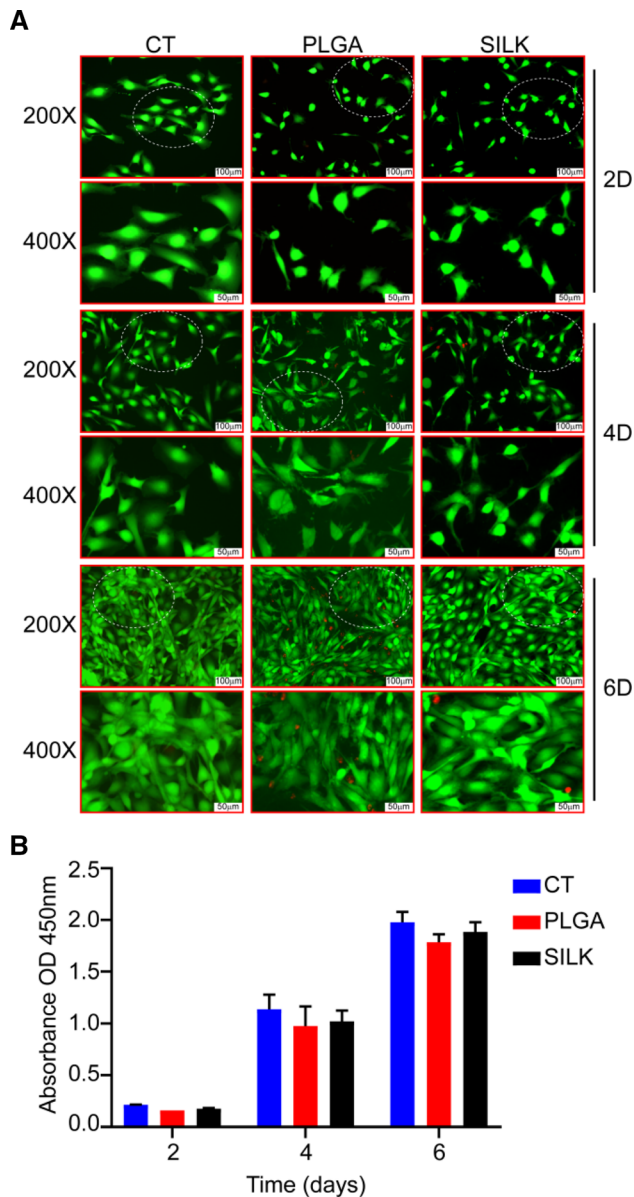


Figure 2 Biocompatibility studies in vitro. **a** 6-day live/dead fluorescence results of the control group, PLGA group, and Silk protein groups. **b** Quantification results of CCK-8 in different groups on the second, fourth, and sixth days. The dotted circle represents the area of the 400X image taken within the 200X image.

by fluorescence microscope (Leica, Wetzlar, Germany).

Observation of long-term antitumor effect: The carry sheet glass adhering with ANM-DSR or blank membrane was soaked in the culture medium, and the medium was changed every 3 days. 786O cells were inoculated at a specific time point (PLGA: 3, 6, 9, 12 days; Silk protein: 6, 12, 18, 24 days) and then

cultured for 1–3 days. The staining steps were as described above.

Cell viability assay

The ANM-DSR and blank membranes were cut into 7*7 mm² slices and adhered to the carry sheet glass. After UV irradiation, the carry sheet glass was placed in 24-well plates. The cells were seeded on the carry sheet glass with a density of 50000 cells per well and cultured for 1–3 days. CCK-8 solution (10%; Meilunbio, Dalian, China) was added to each well and incubated at 37 °C for 1 h. Then transferred the medium to a 96-well plate and the absorbance of 450 nm was measured by a microplate reader (Epoch 2; BioTek, Vermont, USA).

Observation of long-term antitumor effect: the carry sheet glass adhering with ANM-DSR or blank membrane was soaked in the culture medium, and the medium was changed every 3 days. 786O cells were inoculated at a specific time point (PLGA: 3, 6, 9, 12 days; Silk protein: 6, 12, 18, 24 days) and then cultured for 1–3 days. The steps for incubating CCK-8 and measuring absorbance were as above. The staining steps were as described above.

Statistical analyses

The results were expressed as mean ± standard deviation, and all experiments were repeated at least three times. GraphPad Prism version 8.0 (GraphPad Software, San Diego, USA) was used for all statistical analysis. The differences among the control group, blank membrane group, and ANM-DSR group were determined by ANOVA. *P* < 0.05 is considered to be statistically significant.

Results

Preparation of antineoplastic membranes with drug sustained release (ANM-DSRs)

A poly(lactic-co-glycolic acid) (PLGA) and silk protein solution were used in weaving ANM-DSRs. The morphologies of the nanofibers are shown in Fig. 1a, from which two types of nanofibers can be clearly seen. The diameter distribution of the two kinds of ANM-DSRs showed obvious differences (Fig. 1b). The diameter of PLGA nanofibers was a range of 800–1200 nm,

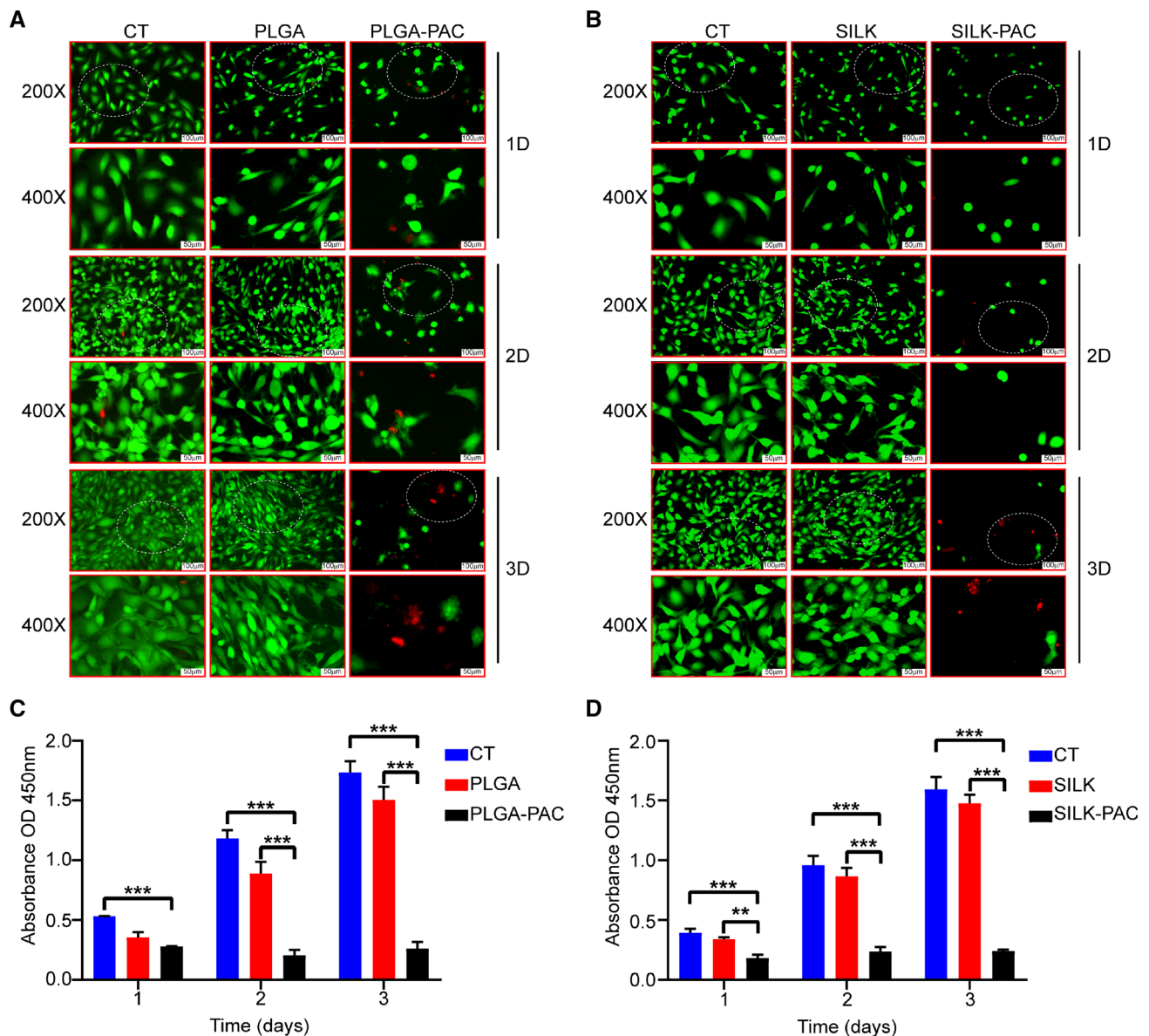


Figure 3 Short-term antitumor effect of ANM-DSRs. **a** 3-day live/dead fluorescence results of the control group, PLGA group, and PLGA-PAC (paclitaxel) group. **b** 3-day live/dead fluorescence results of the control, Silk protein, and SILK-PAC (paclitaxel)

groups. **c, d** Quantification results of CCK-8 in different groups on the first, second, and third days. $**P < 0.01$, $***P < 0.001$. The dotted circle represents the area of the 400X image taken within the 200X image.

whereas the silk protein nanofibers was a range of 250–400 nm. This difference might be attributed to the effect of the PLGA and silk characteristics [38, 39]. The ANM-DSRs of PLGA and silk protein are shown in Figure S1, which appears as a smooth white film.

The UV-vis analysis results indicated that $97.6 \pm 5.6 \mu\text{g}$ of paclitaxel was loaded in each piece of the ANM-DSRs of PLGA, $102.1 \pm 8.1 \mu\text{g}$ of paclitaxel was loaded in each piece of the ANM-DSRs of

silk protein, which was used for subsequent in vitro experiments.

The paclitaxel release profile of ANM-DSRs

The paclitaxel release profile in vitro was detected using the dialysis technique. As shown in Fig. 1c, the results showed two stages. During the first stage, the drug was released in a controlled manner from 0 to 14 days. The cumulative release of ANM-DSRs of

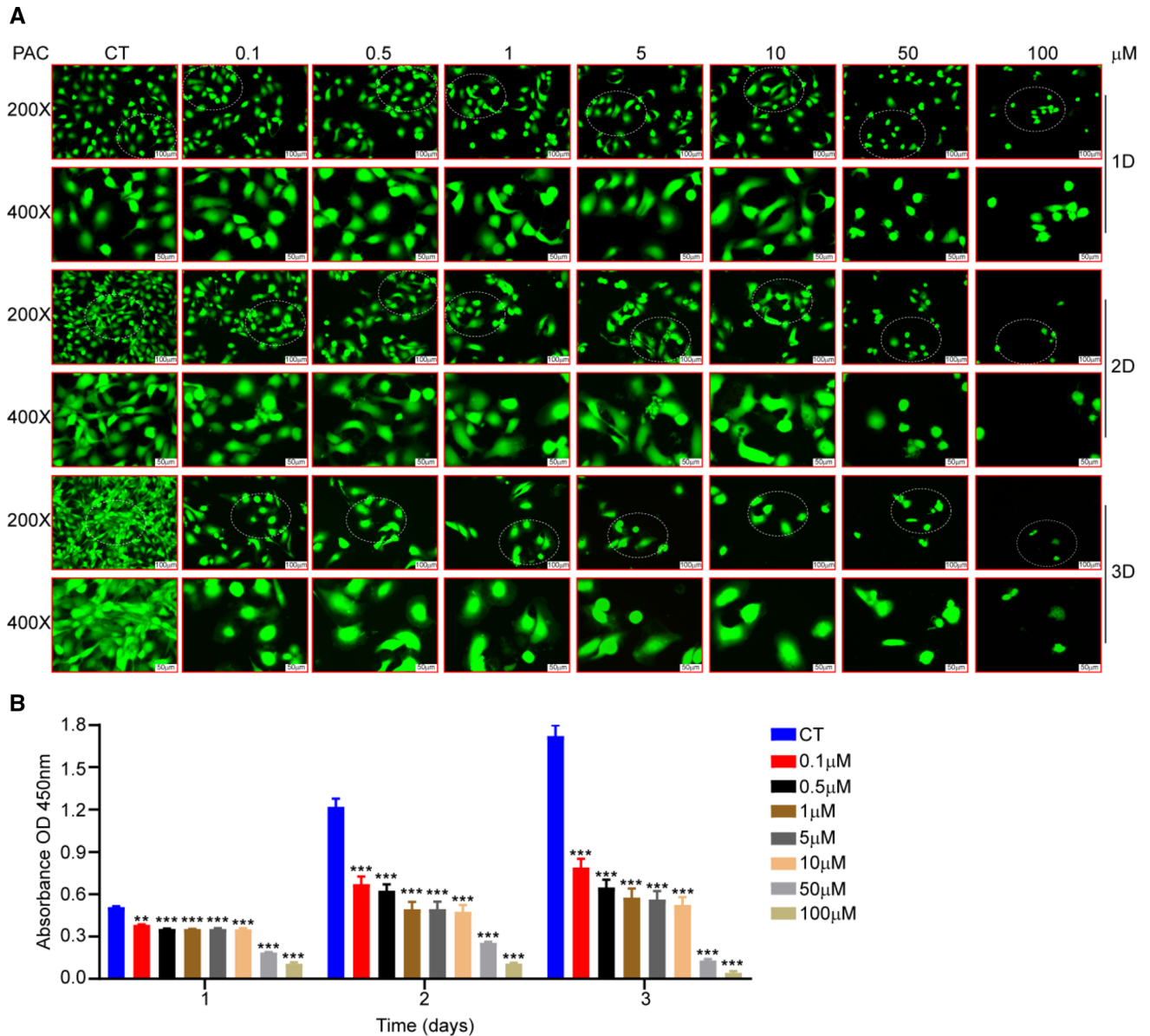


Figure 4 Effect of paclitaxel concentration on 786O cell proliferation. **a** 3-day live/dead fluorescence results of the control group and different concentrations of PAC (paclitaxel) group. **b** Quantification results of CCK-8 in different groups on the

first, second, and third days. $**P < 0.01$, $***P < 0.001$ compared with CT group. The dotted circle represents the area of the 400X image taken within the 200X image.

PLGA was as high as 80%, and that of ANM-DSRs of silk protein was 60%. In the second stage, the drug was released slowly and completely released after 60 days in ANM-DSRs of PLGA and 90 days in ANM-DSRs of silk protein. The ANM-DSRs of PLGA released approximately $26.9 \pm 3.16 \mu\text{g}$ paclitaxel on the first day, while the ANM-DSRs of silk protein released approximately $23.5 \pm 2.93 \mu\text{g}$ paclitaxel (Fig. 1d). The paclitaxel release profile of ANM-DSRs

of PLGA decreased over the next 2 weeks, while that of ANM-DSRs of silk protein lasted for 1 month; both were released slowly over time (Fig. 1d). These results showed that the ANM-DSRs can release a large number of drugs early to meet the needs of short-term and rapid treatment. Yet, the ANM-DSRs can also achieve long-term, continuous treatment and slow down or inhibit tumor recurrence.

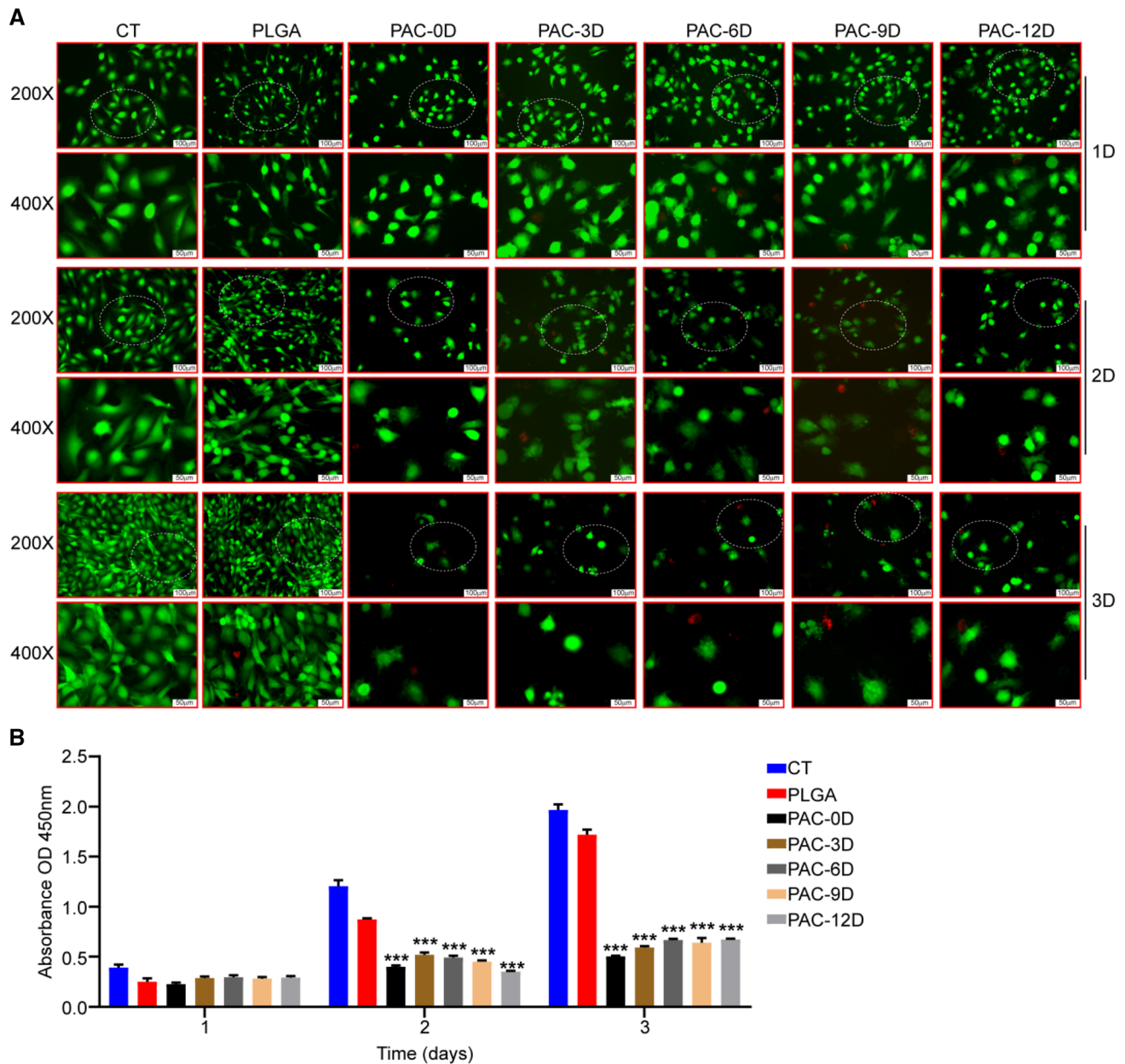


Figure 5 Long-term antitumor effect of the ANM-DSRs of PLGA. **a** 3-day live/dead fluorescence results of the control group, PLGA group, and PLGA-PAC (paclitaxel) group with different immersing times. **b** Quantification results of CCK-8 in different

groups on the first, second, and third days. *** $P < 0.001$ compared with the PLGA group. The dotted circle represents the area of the 400X image taken within the 200X image.

Biocompatibility and short-term antitumor effect of ANM-DSRs

The effect of ANM on the proliferation of the renal clear cell carcinoma cell line 786O was also investigated, as shown in Fig. 2a and b. The results of CCK-8 and fluorescent staining indicated that there were no significant differences among the PLGA, silk protein, and control groups ($P > 0.05$). It is suggested that

PLGA and silk protein have good biocompatibility. Additionally, the short-term, antitumor effects of ANM-DSRs of PLGA and silk protein were evaluated. The ANM-DSRs of PLGA and silk protein showed obvious proliferation inhibition compared to the PLGA, silk protein and control groups (Fig. 3a, b, c and d; 3 days: $P_{\text{PLGA-PAC vs. PLGA}} < 0.001$, $P_{\text{SILK-PAC vs. SILK}} < 0.001$). These results suggest that both the ANM-DSRs of PLGA and silk protein release a large amount

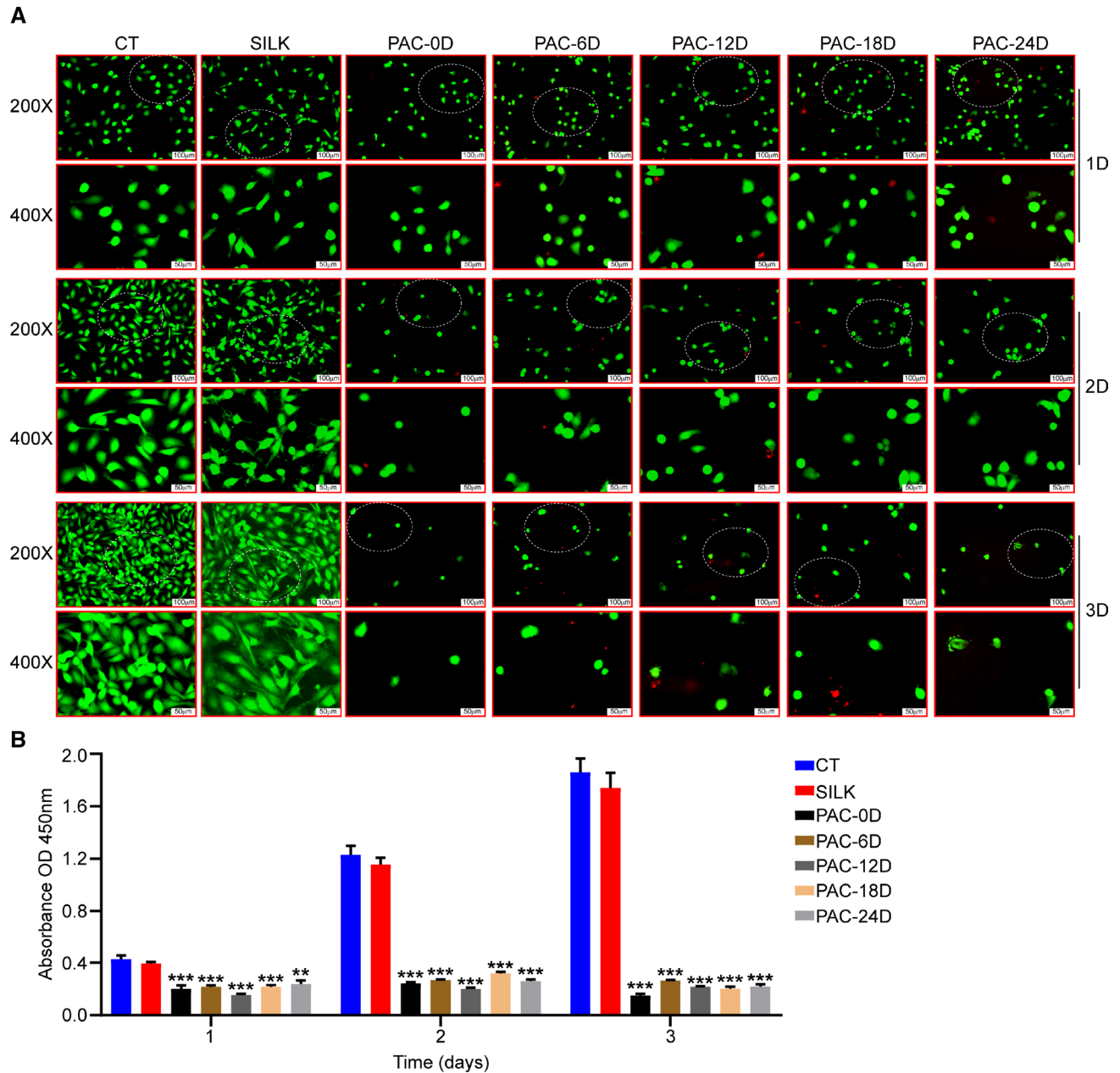


Figure 6 Long-term antitumor effect of the ANM-DSRs of silk protein. **a** 3-day live/dead fluorescence results of the control group, SILK group, and SILK-PAC (paclitaxel) group with different immersing times. **b** Quantification results of CCK-8 in different

groups on the first, second, and third days. ** $P < 0.01$, *** $P < 0.001$ compared with the SILK group. The dotted circle represents the area of the 400X image taken within the 200X image.

of paclitaxel to inhibit tumor growth in the early stage. Furthermore, the effect of paclitaxel concentration on the proliferation of 786O cells was detected, and these results indicated that the higher the paclitaxel concentration, the stronger the inhibitory effect on cell proliferation (Fig. 4a, b, c and d; 3 days: $P < 0.001$).

Long-term antitumor effect of ANM-DSRs

TO evaluate the long-term, antitumor effects of ANM-DSRs of PLGA and silk protein, we soaked the ANM-DSRs in a medium, periodically changed the medium, and implanted the 786O cells after an interval of time. As shown in Fig. 5a, b, the ANM-DSRs of PLGA

appeared to significantly inhibit cell proliferation (3 days: $P_{\text{PAC-0, 3, 6, 9, 12D vs. PLGA}} < 0.001$), and the inhibitory effect did not decrease significantly over time, suggesting that paclitaxel is released slowly and evenly. Similar results were found in the ANM-DSRs of silk protein, they also indicated a significant anti-proliferation effect after soaking for 24 days (Fig. 6a, b; 3 days: $P_{\text{PAC-0, 6, 12, 18, 24D vs. SILK}} < 0.001$). Both results suggest that the sustained release effect of ANM-DSRs of both PLGA and silk protein can allow for long-term, continuous treatment and inhibit tumor recurrence. Notably, the duration of ANM-DSRs of silk protein is longer than that of PLGA.

Discussion

Due to their remarkable properties, electrospun nanofibers have been widely used in a variety of applications ranging from catalysis to environmental protection and biomedicine [30]. Electrospun nanofibers could also be used in cancer chemotherapy by exploiting their ability to encapsulate and release antitumor drugs in a controlled manner. For example, two antitumor agents camptothecin 11 and 7-ethyl-10-hydroxycamptothecin were encapsulated in nanofibers for local delivery, achieving up to 90 days of chemotherapy with significant tumor cytotoxicity against a human colorectal cell line [40]. PLGA and silk protein are two commonly used biomaterials for electrospinning nanofiber liners for controlled anticancer drug delivery [41, 42]. In this study, we used PLGA and silk protein to fabricate two kinds of nanofibers with different diameters by electrospinning and loaded the antitumor drug paclitaxel to achieve a gradient sustained release of paclitaxel and establish a dual-system drug delivery strategy. The prepared nanofibers combine the advantages of both biomaterials. Due to the existence of different properties of PLGA and silk protein and the different sizes of the nanofibers [43, 44], the nanofibers have the characteristics of both short-term release and long-term, sustained release drug therapy, which potentially meets the clinical treatment needs of tumor treatment. At the same time, since renal clear cell carcinoma is insensitive to chemotherapy [45, 46], paclitaxel-loaded nanofibers may achieve a locally high concentration of short-term inhibition of tumor growth and long-term inhibition of tumor recurrence. Combined with the

paclitaxel release data from ANM-DSRs and the inhibition of cell growth, we believe that these nanofibers can achieve rapid drug release in a short period through fine nanofibers and the controlled degraded PLGA components. The subsequent stable and long-term release continues to play an antitumor role, which may be achieved through the slow degradation of thicker nanofibers and the silk protein in the nanofibers. Our results showed that the sustained release of paclitaxel had a lasting inhibitory effect on the proliferation of renal clear cell carcinoma cells. The sustained release membrane has a good antitumor effect and could be used in the treatment of renal clear cell carcinoma. Therefore, it is believed that the naturally derived, gradient release biomaterials provide a new drug delivery strategy for cancer treatment and have great application prospects [47, 48].

Acknowledgements

This work was supported by the National Natural Science Foundation of China (81974392), the Key Laboratory of Guangdong Higher Education Institutes (2021KSYS009), the Guangzhou Key Laboratory of Biological Targeting Diagnosis and Therapy (202201020379), the Guangzhou Core Medical Disciplines Project (2021-2023), the Characteristic Technology Project of Guangzhou Municipal Health Commission (2019TS38), the Guangzhou Key Laboratory Fund (201905010004), the Training Program for Academic Backbone of High Level Universities of Guangzhou Medical University (2017210) and the Key Clinical Specialty Project of Guangzhou Medical University (2020) to Guibin Xu, the National Natural Science Foundation of China (82103359) to Zhiduan Cai, and the Guangzhou Municipal Science and Technology Project (202102020531) to Xiezhao Li.

Author contributions

Conceptualization and design: ZC, LJ, GX; Data curation and formal analysis: All authors; Investigation and Methodology: All authors; Manuscript writing and editing: All authors; Funding acquisition: ZC, XL, GX; Project administration and supervision: LJ, GX.

Declarations

Conflict of interest The authors state that they have no competitive economic interests or personal relationships that may affect the work reported in this paper.

Supplementary Information: The online version contains supplementary material available at <http://doi.org/10.1007/s10853-022-07907-0>.

Open Access This article is licensed under a Creative Commons Attribution 4.0 International License, which permits use, sharing, adaptation, distribution and reproduction in any medium or format, as long as you give appropriate credit to the original author(s) and the source, provide a link to the Creative Commons licence, and indicate if changes were made. The images or other third party material in this article are included in the article's Creative Commons licence, unless indicated otherwise in a credit line to the material. If material is not included in the article's Creative Commons licence and your intended use is not permitted by statutory regulation or exceeds the permitted use, you will need to obtain permission directly from the copyright holder. To view a copy of this licence, visit <http://creativecommons.org/licenses/by/4.0/>.

References

- Bray F, Laversanne M, Weiderpass E, Soerjomataram I (2021) The ever-increasing importance of cancer as a leading cause of premature death worldwide. *Cancer* 127(16):3029–3030
- Sung H, Ferlay J, Siegel RL, Laversanne M, Soerjomataram I, Jemal A, Bray F (2021) Global cancer statistics 2020: GLOBOCAN estimates of incidence and mortality worldwide for 36 cancers in 185 countries. *CA Cancer J Clin* 71(3):209–249
- Siegel RL, Miller KD, Fuchs HE, Jemal A (2021) Cancer statistics 2021. *CA Cancer J Clin* 71(1):7–33
- Hsieh JJ, Purdue MP, Signoretti S, Swanton C, Albiges L, Schmidinger M, Heng DY, Larkin J, Ficarra V (2017) Renal cell carcinoma. *Nat Rev Dis Primers* 3:17009
- Padala SA, Barsouk A, Thandra KC, Saginala K, Mohammed A, Vakiti A, Rawla P, Barsouk A (2020) Epidemiology of renal cell carcinoma. *World J Oncol* 11(3):79–87
- Ljungberg B, Bensalah K, Canfield S, Dabestani S, Hofmann F, Hora M, Kuczyk MA, Lam T, Marconi L, Merseburger AS, Mulders P, Powles T, Staehler M, Volpe A, Bex A (2015) EAU guidelines on renal cell carcinoma: 2014 update. *Eur Urol* 67(5):913–924
- Motzer RJ, Hutson TE, Mccann L, Deen K, Choueiri TK (2014) Overall survival in renal-cell carcinoma with pazopanib versus sunitinib. *N Engl J Med* 370(18):1769–1770
- Motzer R, Alekseev B, Rha S-Y, Porta C, Eto M, Powles T, Grünwald V, Hutson TE, Kopyltsov E, Méndez-Vidal MJ, Kozlov V, Alyasova A, Hong S-H, Kapoor A, Alonso Gordo T, Merchan JR, Winquist E, Maroto P, Goh JC, Kim M et al (2021) Lenvatinib plus pembrolizumab or everolimus for advanced renal cell carcinoma. *N Engl J Med* 384(14):1289–1300
- Choueiri TK, Powles T, Burotto M, Escudier B, Boursin MT, Zurawski B, Oyervides Juárez VM, Hsieh JJ, Basso U, Shah AY, Suárez C, Hamzaj A, Goh JC, Barrios C, Richardet M, Porta C, Kowalyszyn R, Feregrino JP, Żołnierek J, Pook D et al (2021) Nivolumab plus cabozantinib versus sunitinib for advanced renal-cell carcinoma. *N Engl J Med* 384(9):829–841
- Zhu L, Chen L (2019) Progress in research on paclitaxel and tumor immunotherapy. *Cell Mol Biol Lett* 24:40
- Jotte R, Cappuzzo F, Vynnychenko I, Stroyakovskiy D, Rodríguez-Abreu D, Hussein M, Soo R, Conter HJ, Kozuki T, Huang K-C, Graupner V, Sun SW, Hoang T, Jessop H, Mcclelland M, Ballinger M, Sandler A, Socinski MA (2020) Atezolizumab in combination with carboplatin and nab-paclitaxel in advanced squamous NSCLC (IMpower131): results from a randomized phase III trial. *J Thorac Oncol* 15(8):1351–1360
- Fader AN, Roque DM, Siegel E, Buza N, Hui P, Abdelghany O, Chambers S, Secord AA, Havrilesky L, Malley DM, Backes FJ, Nevadunsky N, Edraki B, Pikaart D, Lowery W, Elshawi K, Celano P, Bellone S, Azodi M, Litkouhi B et al (2020) Randomized phase II trial of carboplatin-paclitaxel compared with carboplatin-paclitaxel-trastuzumab in advanced (stage III–IV) or recurrent uterine serous carcinomas that overexpress her2/neu (NCT01367002): updated overall survival analysis. *Clin Cancer Res* 26(15):3928
- Weaver BA (2014) How taxol/paclitaxel kills cancer cells. *Mol Biol Cell* 25(18):2677–2681
- Rowinsky EK, Cazenave LA, Donehower RC (1990) Taxol: a novel investigational antimicrotubule agent. *J Natl Cancer Inst* 82(15):1247–1259
- Rahnfeld L, Luciani P (2020) Injectable lipid-based depot formulations: where do we stand? *Pharmaceutics* 12(6):567
- Lee JH, Moon M, Kim Y-C, Chung SJ, Oh J, Kang DY, Lee S-Y, Lee K-H, Yun J, Kang H-R (2020) A one-bag rapid

- desensitization protocol for paclitaxel hypersensitivity: a noninferior alternative to a multi-bag rapid desensitization protocol. *J Allergy Clin Immunol Pract* 8(2):696–703
- [17] Feldweg AM, Lee C-W, Matulonis UA, Castells M (2005) Rapid desensitization for hypersensitivity reactions to paclitaxel and docetaxel: a new standard protocol used in 77 successful treatments. *Gynecol Oncol* 96(3):824–9
- [18] Miele E, Spinelli GP, Miele E, Tomao F, Tomao S (2009) Albumin-bound formulation of paclitaxel (Abraxane ABI-007) in the treatment of breast cancer. *Int J Nanomed* 4:99
- [19] Namgung R, Mi Lee Y, Kim J, Jang Y, Lee B-H, Kim I-S, Sokkar P, Rhee YM, Hoffman AS, Kim WJ (2014) Polycyclodextrin and poly-paclitaxel nano-assembly for anti-cancer therapy. *Nat Commun* 5:3702
- [20] Niiyama E, Uto K, Lee CM, Sakura K, Ebara M (2019) Hyperthermia nanofiber platform synergized by sustained release of paclitaxel to improve antitumor efficiency. *Adv Healthc Mater* 8(13):e1900102
- [21] Li Z, Zhang X, Guo Z, Shi L, Jin L, Zhu L, Cai X, Zhang J, Zhang YS, Li J (2021) Nature-derived bionanomaterials for sustained release of 5-fluorouracil to inhibit subconjunctival fibrosis. *Mater Today Adv* 11:100150
- [22] Chen Y, Shen W, Tang C, Huang J, Fan C, Yin Z, Hu Y, Chen W, Ouyang H, Zhou Y, Mao Z, Chen X (2020) Targeted pathological collagen delivery of sustained-release rapamycin to prevent heterotopic ossification. *Sci Adv* 6(18):eaay9526
- [23] Danhier F, Ansorena E, Silva JM, Coco R, Le Breton A, Préat V (2012) PLGA-based nanoparticles: an overview of biomedical applications. *J Control Release Off J Control Release Soc* 161(2):505–522
- [24] Acharya S, Sahoo SK (2011) PLGA nanoparticles containing various anticancer agents and tumour delivery by EPR effect. *Adv Drug Deliv Rev* 63(3):170–183
- [25] Vert M, Mauduit J, Li S (1994) Biodegradation of PLA/GA polymers: increasing complexity. *Biomaterials* 15(15):1209–1213
- [26] Huang W, Ling S, Li C, Omenetto FG, Kaplan DL (2018) Silkworm silk-based materials and devices generated using bio-nanotechnology. *Chem Soc Rev* 47(17):6486–6504
- [27] Wang Z, Yang Z, Jiang J, Shi Z, Mao Y, Qin N, Tao TH (2021) Silk microneedle patch capable of on-demand multi-drug delivery to the brain for glioblastoma treatment. *Adv Mater Deerfield Beach Fla* 34:e2106606
- [28] Chambre L, Martín-Moldes Z, Parker RN, Kaplan DL (2020) Bioengineered elastin- and silk-biomaterials for drug and gene delivery. *Adv Drug Deliv Rev* 160:186–198
- [29] Han C, Zhou J, Liu B, Liang C, Pan X, Zhang Y, Zhang Y, Wang Y, Shao L, Zhu B, Wang J, Yin Q, Yu X-Y, Li Y (2019) Delivery of miR-675 by stem cell-derived exosomes encapsulated in silk fibroin hydrogel prevents aging-induced vascular dysfunction in mouse hindlimb. *Mater Sci Eng C Mater Biol Appl* 99:322–332
- [30] Xue J, Wu T, Dai Y, Xia Y (2019) Electrospinning and electrospun nanofibers: methods, materials, and applications. *Chem Rev* 119(8):5298–5415
- [31] Yang G, Li X, He Y, Ma J, Ni G, Zhou S (2017) From nano to micro to macro: electrospun hierarchically structured polymeric fibers for biomedical applications. *Progress Polym ence* 81:80–113
- [32] Qi R-L, Tian X-J, Guo R, Luo Y, Shen M-W, Yu J-Y, Shi X-Y (2016) Controlled release of doxorubicin from electrospun MWCNTs/PLGA hybrid nanofibers. *Chin J Polym Sci* 34(9):1047–1059
- [33] Wu H, Liu S, Xiao L, Dong X, Lu Q, Kaplan DL (2016) Injectable and pH-responsive silk nanofiber hydrogels for sustained anticancer drug delivery. *ACS Appl Mater Interfaces* 8(27):17118–17126
- [34] Chen Z, Zhuang Q, Cheng K, Ming Y, Zhao Y, Ye Q, Zhang S (2020) Long non-coding RNA TCL6 enhances preferential toxicity of paclitaxel to renal cell carcinoma cells. *J Cancer* 11(6):1383–1392
- [35] Rausch M, Weiss A, Achkhanian J, Rotari A, Nowak-Sliwinska P (2020) Identification of low-dose multidrug combinations for sunitinib-naive and pre-treated renal cell carcinoma. *Br J Cancer* 123(4):556–567
- [36] Chua CYX, Ho J, Demaria S, Ferrari M, Grattoni A (2020) Emerging technologies for local cancer treatment. *Adv Ther* 3(9):2000027
- [37] Kesharwani P, Tekade RK, Jain NK (2011) Spectrophotometric estimation of paclitaxel. *Int J Adv Pharm Sci* 2(1):29–32
- [38] Pourtalebi Jahromi L, Ghazali M, Ashrafi H, Azadi A (2020) A comparison of models for the analysis of the kinetics of drug release from PLGA-based nanoparticles. *Heliyon*. 6(2):e03451
- [39] Solomun JI, Totten JD, Wongpinyochit T, Florence AJ, Seib FP (2020) Manual versus microfluidic-assisted nanoparticle manufacture: impact of silk fibroin stock on nanoparticle characteristics. *ACS Biomater Sci Eng* 6(5):2796–2804
- [40] Yohe ST, Herrera VL, Colson YL, Grinstaff MW (2012) 3D superhydrophobic electrospun meshes as reinforcement materials for sustained local drug delivery against colorectal cancer cells. *J Control Release* 162(1):92–101
- [41] Kim K, Luu YK, Chang C, Fang D, Hsiao BS, Chu B, Hadjiargyrou M (2004) Incorporation and controlled release of a hydrophilic antibiotic using poly(lactide-co-glycolide)-based electrospun nanofibrous scaffolds. *J Control Release* 98(1):47–56
- [42] Laiva AL, Venugopal JR, Karuppuswamy P, Navaneethan B, Gora A, Ramakrishna S (2015) Controlled release of

- titanocene into the hybrid nanofibrous scaffolds to prevent the proliferation of breast cancer cells. *Int J Pharm* 483(1):115–123
- [43] Minoura N, Tsukada M, Nagura M (1990) Physico-chemical properties of silk fibroin membrane as a biomaterial. *Biomaterials* 11(6):430–434
- [44] Abbasnezhad N, Zirak N, Shirinbayan M, Tcharkhtchi A, Bakir F (2021) On the importance of physical and mechanical properties of PLGA films during drug release. *J Drug Deliv Sci Technol* 63:102446
- [45] Li S, Yang J, Wang J, Gao W, Ding Y, Ding Y, Jia Z (2018) Down-regulation of miR-210-3p encourages chemotherapy resistance of renal cell carcinoma via modulating ABCC1. *Cell Biosci* 8(1):9
- [46] Kakehi Y, Kanamaru H, Yoshida O, Ohkubo H, Nakanishi S, Gottesman MM, Pastan I (1988) Measurement of multidrug-resistance messenger RNA in urogenital cancers; elevated expression in renal cell carcinoma is associated with intrinsic drug resistance. *J Urol* 139(4):862–865
- [47] Li Z, Huang J, Wu J (2021) pH-sensitive nanogels for drug delivery in cancer therapy. *Biomater Sci* 9(3):574–589
- [48] Tong X, Pan W, Su T, Zhang M, Dong W, Qi X (2020) Recent advances in natural polymer-based drug delivery systems. *React Funct Polym* 148:104501

Publisher's Note Springer Nature remains neutral with regard to jurisdictional claims in published maps and institutional affiliations.

Springer Nature or its licensor (e.g. a society or other partner) holds exclusive rights to this article under a publishing agreement with the author(s) or other rightsholder(s); author self-archiving of the accepted manuscript version of this article is solely governed by the terms of such publishing agreement and applicable law.